Maximizing Signal-to-Noise Ratio in TaO Laser Induced Fluorescence Spectroscopy

T. Conibear[a)]

(Dated: 3 December 2020)

Various methods to improve the signal of fluorescence photons in Laser Induced Fluorescence (LIF) spectroscopy and reduce detection noise, such as scattered excitation laser photons, are discussed to maximize signal-to-noise ratio. Final estimations of the number of fluorescence photons collected per experimental shot is 30, while the number of background photons is less than one, within a detection frame of 10 μs. Fast gate switching the photomultiplier tube (PMT) is the most critical step to reduce the background and maximize the signal-to-noise ratio. A designed detection cube also greatly increases solid angle covered by the PMT detector, thereby improving detection efficiency.

I. INTRODUCTION

When atoms or molecules absorb energy, they enter excited states. These excited states primarily manifest themselves in electrons in the outermost shells or states, called valence electrons. A valence electron's most stable condition is at a ground state, more easily referred to as S_0, but when excited, a valence electron enters a higher energy state like S_1 or S_2. This new condition is inherently unstable, so the electron quickly transitions, or relaxes, back to its ground state in a process called spontaneous decay. During this process, an electron emits the excess energy gained in the form of a photon, called fluorescence. Due to quantization of energy states, fluorescence emissions occur over a discrete range, or spectrum and each species of atom or molecule has a unique emission spectrum.

Excited electrons can decay to intermediate states before returning to the ground state. Therefore, an excited electron can emit multiple photons during its spontaneous decay process. Emission of multiple photons with different wavelength by one atom is evidence of multiple transitions and states within the electronic structure. Analyzing an atom's emission spectrum can reveal much about specific atomic or molecular electronic structure and behavior.

By placing an atom in a radiation field such as a laser, electronic excitation can be induced as photons from the radiation field are absorbed by the atom.[1] This process is called induced absorption. An atom's susceptibility toward induced absorption is determined by its electronic structures of the initial and final states. This susceptibility is quantitatively given by the Einstein coefficient of induced absorption, B_{12}, which is primarily determined by the transition moment. Induced absorption can be used to populate desired states by tuning laser wavelength to resonate at the transition frequency.

Excitation from induced absorption necessitates fluorescence. Emissions occur via two processes: stimulated or spontaneous emissions.[1,2] Stimulated emission occurs when the excitation field itself induces the excited electron to transition to a lower energy state and emit a photon. The emitted photon is in the same mode as what caused its emission, meaning it has the same frequency and direction. B_{21} is the constant factor called the Einstein coefficient of stimulated emission. B_{21} has time symmetry with induced absorption and is thereby dependent on B_{12}. They are related by $B_{12} = B_{21}\frac{g_1}{g_2}$, where g represents the degeneracy of the two states. Thus, B_{12} is equal to B_{21} when the two state's degeneracy is equal.

Separately, spontaneous emission does not require an external field.[1,2] This means it lacks resonant selectivity as well. The final states and relaxation rate are completely determined by A_{21}, the Einstein coefficient of spontaneous emission. A_{21} is equal to $(\hbar\omega_{21}^3/\pi^2c^3)B_{21}$, where ω_{21}^3 is the transition frequency between the two states. Therefore, A_{21} is dependent on transition frequency, not the surrounding radiative field.

All three processes culminate in a rate equation governing the population of a certain state. The Einstein rate equation is $\frac{dN_2}{dt} = B_{12}u_\nu N_1 - B_{21}u_\nu N_2 - A_{21}N_2$, where u_ν is a constant determined by spectral energy density of the radiative field. Again, spontaneous emission is unrelated to the surrounding radiative field as it lacks the u_ν term, while induced absorption and stimulated emission are directly influenced by it.

Induced absorption and subsequent processes of stimulated and spontaneous emission are utilized in laser-induced fluorescence (LIF). LIF involves directing a laser at a gaseous substance and detecting resulting fluorescence emissions.[3] Excitation lasers are usually narrow band and capable of being tuned to specific wavelengths which induce desired electronic transitions. A photo-multiplier tube (PMT), is typically used to collect fluorescence photons.Because of the sensitivity, simplicity and high spectroscopic resolution, LIF has considerable application in studying molecular electronic structures. In our lab, LIF is apt to study tantalum oxide (TaO), a molecule with inherent characteristics suited to explore physics beyond the Standard Model.

Because a typical electric-dipole transition of TaO has a small absorption cross-section, a high power pulsed laser is implemented for excitation. This introduces significant noise in detection of fluorescence photons as laser photons are scattered within the apparatus. And because fluorescence occurs isotropically from the source, effort must also be made to have fluorescence photons directed toward the PMT to boost signal. Thus, the primary experimental focus is improving the signal-to-noise ratio to speed up the data collection process. Various methods and techniques are employed into the experimental apparatus and data analysis to reduce noise and improve fluorescence photon signals.

[a)]Physics and Astronomy Department, UNLV.

II. THEORETICAL BACKGROUND

A. Fluorescence Transitions and Emission

Intensity of specific spectral lines not only depends on population density of specific absorbing or emitting states, but also on the probability a specific molecular transition will occur.[1] Transition probabilities are related to an atom's Einstein coefficient of spontaneous emission. The probability, P, an excited molecule in E_i makes a transition to a lower energy level E_k is given by:

$$\frac{dP_{ik}}{dt} = A_{ik}, \tag{1}$$

where A_{ik} is the Einstein coefficient of spontaneous emission from E_i to E_k. The photon emitted in this transition has frequency equal to $(E_i - E_k)/h$. Because several energy states less than E_i often exist, total transition probability is:[1]

$$A_i = \sum_k A_{ik}. \tag{2}$$

Figure 1 shows energy levels lower than E_i and their associated Einstein coefficients. Each transition represents a unique photon emission. Excited molecules at E_i can also change energy via collisions.[1,3] These collision induced energy states are shown in Fig. 1, and their probability is given by the radiationless transition rate, R_k.

However, gaseous molecules that aren't compressed, especially those in a vacuum, do not collide enough to make these energy states a significant consideration. Specifically, excited diatomic gas molecules like TaO spontaneously transition from E_i to several lower states before reaching the stable condition as direct transitions to the ground state have low transition frequencies. Consequently, an excited molecule emits multiple photons during its fluorescence process. Stimulated emission of photons is assumed to be negligible within the experiment because it occurs when the excitation field is intense, a condition actively avoided in the experiment to avoid power broadening. Stimulated emissions that do occur will emit in the same direction as excitation laser photons, further reducing their effect on detected signal. Therefore, all fluorescence photons are assumed to be spontaneous emissions.

The number of initial states is determined by temperature. Higher temperatures increase the number of initial populated states. Consequently, there can be significant overlap of spectral lines and determining which line corresponds to a certain transition becomes difficult. To reduce additional energy levels and complexity of the spectra, the temperature of target molecules is significantly reduced to a few Kelvin through a supersonic nozzle to a vacuum. Therefore, only several quantum states which are heavily populated exist. Reducing temperature also reduces the number of collisions, thereby minimizing collision induced radiationless transitions.

In LIF, the emitted photon rate, n_f can be calculated from the number of photons absorbed per second, n_a, which is given by:[3]

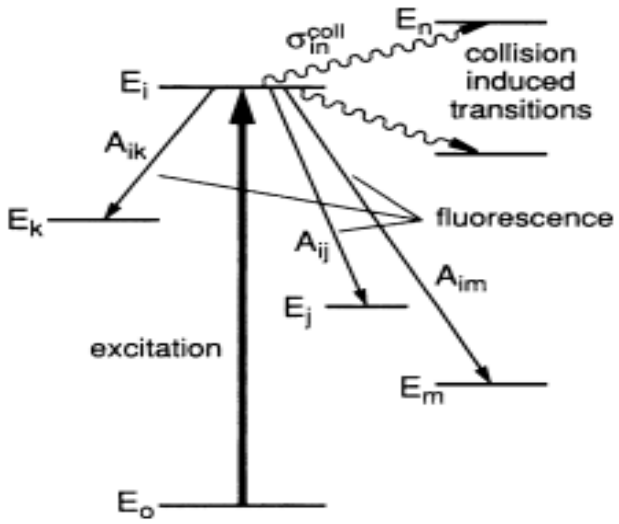

FIG. 1. Fluorescence and collision induced transitions of an excited state, E_i.[1]

$$n_a = N_0 \cdot n_L \cdot \sigma \cdot \Delta x, \tag{3}$$

where Δx is the path length, n_L is the number of incident laser photons per second, σ is the molecular absorption cross section, and N_0 is the density of molecules in the absorbing state.

An excited state transitions through spontaneous emission or collision induced radiationless transitions. But, the number of fluorescence photons is reduced relative to excited atoms if the radiationless transition probability R_k is greater than zero. Therefore, the quantum efficiency of the excited state, η_k, represents the likelihood a transition to a given state emits a photon. η_k is equal to $A_i/(A_i + R_k)$. The number of fluorescence photons emitted per second is:

$$n_f = \eta_k \cdot n_a. \tag{4}$$

If η_i is equal to one then the number of fluorescence photons emitted per second is equal to the number of laser photons absorbed per second. It also means the radiationless transition probability is equal to zero. This is assumed to be the case in experimental conditions of low temperature and gaseous TaO.

B. Solid Angle

Understanding the likelihood that photons emerge toward a given region from a fluorescence event involves the use of solid angle. Excited molecules are assumed to have random spatial distribution, resulting in fluorescence photons emitting isotropically.[1] So, photons can be conceived as existing on a sphere of radius r that grows as they move from the fluorescence source, with polar angles θ and ϕ specifying direction.[4] A narrow, circular cone around θ and ϕ, with its apex at the

source, is used to intersect the sphere. This cone intersects a spherical surface with area A, which is proportional to r^2. The solid angle of the cone, $\Delta\Omega$, is then defined as:

$$\Delta\Omega = \frac{A}{r^2}, \tag{5}$$

with units of steradians (sr). Thus, since the area of a whole sphere is $4\pi r^2$, its solid angle would be 4π sr. So, solid angle of a given area decreases as its distance, or radius, from photon emission increases. This is expected as the random motion and direction of photons have more ability to move away from a given area the further they have to travel to it.

A detector cannot be placed around the entire sphere about a fluorescence event, so maximizing an apparatus' solid angle is necessary to maximize detection efficiency. This can be achieved by increasing area of detectors such as a PMT, or placing the PMT as near the fluorescence event as possible. But placement of a PMT must also be balanced with minimization of noise from excitation laser photons. Therefore, the experimental PMT is placed in an optical apparatus consisting of mirrors, lenses, and tubes to simultaneously minimize noise and maximize fluorescence photon detection within the parameters set by the vacuum chamber system.

C. Photomultiplier Tube

A photomultiplier tube detects emitted photons, then amplifies and converts the photon current signal to a mV level voltage signal that is recorded by a fast oscilloscope. Typical PMTs utilize a series of electron multipliers called dynodes.[5,6] An incident photon strikes a photocathode, producing a photoelectron. Then an electric field accelerates the photoelectron while an electrode ensures its path is focused toward a dynode. Because it is accelerated, the photoelectron possesses enough energy that it frees other electrons upon striking the dynode surface. The original photoelectron and secondary electrons are directed toward another dynode and an accelerating voltage is again present, prompting emission of even more electrons upon collision. This secondary emission process is repeated on numerous dynodes, developing a cascading effect which results in hundreds of thousands electrons being detected at the anode. Thus, a single photon impinging on the PMT can produce a stronger current capable of being reported by an oscilloscope with an appropriate input impedance.

The approximate number of electrons produced per incident photon is called gain. And because the PMT relies on random electron collisions, gain is not always constant. Gain can be increased by adding dynodes, optimizing secondary electron trajectory, and increasing the accelerating electric field via applied voltage. Also, to prevent noise from external electron emission or detection, the PMT apparatus is contained within a vacuum tube.

Another type of PMT utilizes micro-channel plates for electron multiplication. A micro-channel plate consists of many small, micrometer sized through-holes. Electron multiplication begins if a photoelectron enters a hole. A MCP-PMT can contain several multi-channel plates, increasing electron gain with each added plate. A MCP-PMT is designed for fast response (<100 ps compared to 3 ns with regular dynode PMTs), rendering it useful for fast photon counting.

An approximation of a PMTs resulting oscilloscope signal can be performed using its typical gain and anode pulse rise time. Current is found by multiplying an incident photon by the typical gain, g, and then dividing by pulse rise time, Δt, which is the time it takes for all anode current to be discharged toward the oscilloscope. Then, anode current is converted to voltage using Ohm's law, V=IR, where R is the input impedance of the oscilloscope and the final equation is:

$$V = \left(\frac{1 \cdot g \cdot q}{\Delta t}\right) R, \tag{6}$$

where q is electron charge of $1.602 \cdot 10^{-19}$ C. Pulse rise time is influenced by PMT design, with MCP-PMTs being faster than regular PMTs. It is also influenced by output impedance. Lower output impedances allow current to move faster, decreasing pulse width, while larger impedances slow current and widen resulting pulses, but generate larger voltage signals.

III. SIGNAL AND NOISE ANALYSIS

Primary influences on detected LIF signal are PMT efficiency, PMT solid angle, excitation efficiency, and total number of molecules populating each state. The most significant source of noise is scattered excitation laser photons, while the dark current of the PMT and oscilloscope also must be considered. Improving the signal-to-noise ratio means maximizing features which improve signal while minimizing those that provide noise, and is the primary experimental objective.

A. Effects on PMT Signal

The efficiency of both dynode and MCP photomultiplier tubes is not 100%. A photon is not guaranteed to generate a photoelectron upon striking the photoelectron plate. More specifically, PMT efficiency is described by photocathode quantum efficiency, η_{ph}, which is the ratio of photoelectrons produced to photons impinging upon the photocathode, or $\eta_{ph} = n_{pe}/n_{ph}$.[3] Generally, η_{ph} is 10 to 30 percent, indicating significant signal loss. The solid angle covered by the PMT also impacts efficiency of fluorescence photon detection. The fraction of total fluorescence photons collected, δ, is equal to the systems solid angle divided by total solid angle 4π, or $\delta = \Delta\Omega/4\pi$. The number of counted photons per second becomes:

$$n_{pe} = n_a \cdot \eta_k \cdot \eta_{ph} \cdot \delta. \tag{7}$$

This equation can be applied to experimental devices and conditions to estimate counted photon signal. η_{ph} is an inherent quality of a PMT, so it cannot be changed. The typical η_{ph}

of the experimental PMT is between 14% and 30%, depending on wavelength, but is taken to be 20% for estimation. δ is improved by collecting more fluorescence photons with optical components like lenses and mirrors. Experimental solid angle, explained in Experimental Methods, is approximately 4.01 ± 0.29 sr, resulting in 31.87% efficiency.

However, there is added inefficiency from lenses and mirrors as they do not transmit or reflect all incident photons. Experimentally, average signal loss at the reflector mirror is 10%, and 5% is estimated at each interface of the entry Brewster window, lenses, and PMT window, totalling eight interfaces. Thus, experimental detection loss is estimated to be 50%.

η_k is inherent to a given excited state, but is assumed to be one due to the low temperature and gaseous nature of TaO molecules. n_a is influenced by the population of an energy state. In this experiment, the number of molecules at any given state is conservatively estimated to be $1 \cdot 10^4$. Total molecular number is random, depending on the effectiveness of laser ablation and the surrounding gas mixture in creating TaO. As the experiment is conducted, total molecular number will increase as these features are optimized.

However, the number of molecules actually excited in a state is determined by excitation efficiency. The number of excited TaO molecules per laser pulse can be increased if the laser is more intense.[7] However, increasing excitation laser intensity broadens the range of spectral lines produced by target atoms. Called power broadening, this phenomenon decreases frequency resolution. Consequently, excitation efficiency is purposely reduced to 10% to ensure power broadening is not an issue. Laser beam width also impacts excitation efficiency.

The number of fluorescence photons detected per shot is estimated by applying Eq. 7 and additional efficiencies. Excitation efficiency of 10% is applied to the molecular number within a given quantum state of $1 \cdot 10^4$, resulting in 1000 excited molecules which emit photons. Then, solid angle efficiency, interface detection losses, and photocathode quantum efficiency are applied, yielding approximately 30 photons per shot within a total detection frame of 10 μs. Consequently, the average number of photons counted within several seconds is much larger. Table I shows the influences on signal and their respective efficiencies.

B. Noise and its Reduction

Scattered photons from the excitation laser are the largest source of noise. Estimations of how many scattered excitation laser photons must be reduced to improve the signal to noise ratio begins with the energy of the laser pulse. Each pulse will have energy of 10 μJ. Using the Planck-Einstein relation E=Nhν, and substituting the electromagnetic radiation relation c=$\lambda\nu$ for ν, the number of photons per shot, N, is determined. If λ is 500 nm, then N is $2.517 \cdot 10^{13}$ photons. And though the exact number of photons scattered each pulse is random, it is orders of magnitude greater than the number of fluorescence photons detected per pulse.

TABLE I. Influences on signal and their efficiency.

Influences	Efficiency %
Excitation Efficiency	10
Solid Angle	31.87
Detection Loss	50
Photocathode Efficiency	20

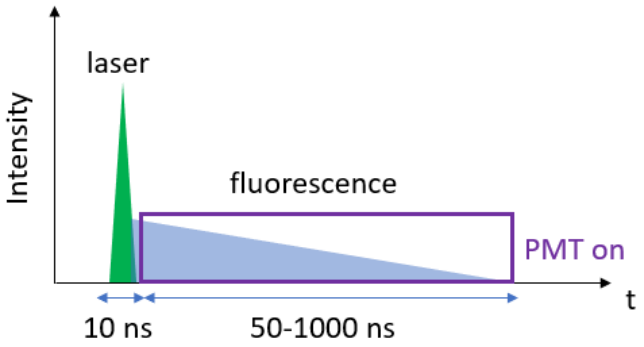

FIG. 2. Example of PMT gating.

A simple solution commonly used to reduce noise is a color filter or long-pass filter, which can be placed in front of the PMT to filter out excitation laser photons. A color filter can reduce the number of unwanted photons by $1 \cdot 10^6$, but its bandwidth blocks certain fluorescence photons and reduces signal efficiency. It specifically blocks emissions from fluorescence transitions to a ground state, as they are incredibly similar to the excitation laser wavelength. Since all transitions of TaO are of experimental interest, a color filter is not used. Furthermore, a color filter's effectiveness changes with wavelength, so a filter will have to be constantly changed as the laser wavelength is tuned—a time consuming and expensive action in an apparatus within a vacuum chamber.

The primary PMT feature to improve signal accuracy is a gate. When the gate is on, an electric field is produced which prevents initial photoelectrons from colliding with a dynode or MCP. If the gate is off, a PMT functions like normal and the electric field accelerates photoelectrons. A gate can be rapidly turned on or off in a process called gate switching. Desired frequency of gate switching depends on laser pulse duration. Since most lasers have nanosecond scale pulses, fast gate switching on the order of nanoseconds is needed as well. The speed of gate switching is the biggest determinant of a gate's effectiveness at reducing noise.

Gate switching reduces unwanted signal from laser photons by preventing PMT detection until the laser pulse has fired. In doing so fluorescence photons compose the majority of signal detected by the PMT. Because fluorescence does not occur instantaneously, the gate can be turned off some time after the laser has fired, allowing more laser photons to exit the detection area. During this time lag, the number of laser photons decreases while fluorescence begins to occur and the population of their photons increases. Therefore, signal noise produced by laser photons is reduced as they are undetected while the PMT gate is on. However, the time lag depends on the

desired fluorescence photons, as smaller wavelength photons (UV) fluoresce faster than longer wavelength photons (IR). Ideally, the time lag is large enough to allow all excitation laser photons to exit; but since fluorescence occurs incredibly fast, the time lag must be balanced to maximize fluorescence photon detection relative to laser photons. Fast gating is visually represented in Fig. 2, where the gate is turned on after a brief time lag to reduce intensity of excitation photons and allow fluorescence photons to populate.

Most commercial MCP-PMTs come equipped with fast gating. However, regular PMTs do not usually possess a gating capability and continuously detect signal. Consequently, dynode PMTs are not preferable for our pulsed LIF applications. But a circuit triggering fast gating effects can be constructed and applied to a dynode PMT. Instead of cutting off accelerating voltage applied to all dynodes, a gate is instead applied to the first dynode.

After PMT gating, the number of detected scattered excitation laser photons is expected to be reduced by $1{\cdot}10^8$ per shot. Consequently, background is expected to be less than one photon per shot. Signal noise is also introduced from PMT dark current of 10 nA and inherent noise from the oscilloscope. This noise is addressed by photon counting methods.

IV. EXPERIMENTAL METHODS

A system designed to maximise detection of fluorescence photons from TaO and minimize detection of scattered photons from the excitation laser was constructed. TaO molecules are created via laser ablation of a tantalum rod within a gaseous mixture containing oxygen. Because ablation creates molecules at a high temperature, they must be cooled to reduce the number of electronic states and improve experimental accuracy and reliability. Cooling to several Kelvin occurs via the supersonic nozzle which also accelerates TaO molecules as a beam into the fluorescence chamber vacuum. The detection chamber is a stainless steel vacuum chamber at 10^{-7} torr. Upon entering the chamber, a tunable, five to ten ns pulsed excitation laser strikes the molecule beam at 90° within the detection chamber. Resulting fluorescence photons are collected by optical components and focused onto a PMT. Detection will occur over approximately 10 μs as the largest fluorescence lifetime of experimental interest is several μs.

Because PMTs need to accelerate photoelectrons, they require a large negative power supply of up to -5 kV. Traditional power supplies do not provide this magnitude of voltage. A negative high voltage power supply was constructed using an EMCO C50N programmable power supply. It's maximum output is -5 kV. Special considerations needed to be made such that power was input prior to programming commands. This was accomplished by putting an LED in parallel with power input so the LED is on when power is applied. A manual switch is used to apply programming inputs. The switch is always turned off if the LED is off so that programming inputs are not applied before power inputs. A National Instruments Digital Acquisition (DAQ) board provides programming inputs for the C50N.

A. Detection Cube

The detection system is centered around a cube with holes on each face. Initially, designs were centered around a commercial ThorLabs optical cube, but it was found unable to be fit inside the vacuum chamber. A smaller cube was then designed on SolidWorks and machined. Two directly opposite faces contain holes with SM2 threading for ThorLabs lens tubes while the remaining sides contain unthreaded holes to allow the excitation laser and TaO molecules to enter and exit. Lens tubes are necessary to hold photon collection optical components.

The first lens tube contains an Edmunds Optics concave mirror with 50 mm diameter and 25 mm focal length. Its purpose is to act as a reflector mirror, reflecting fluorescence emissions back toward the middle of the cube and the opposing side's lens tube which contains two lenses. The first lens is an Edmunds Optics aspheric condenser lens with 50 mm diameter and back focal length of 24.7 mm; it has the purpose of collecting and collimating incident fluoresence photons. These collimated photons then travel down the tube toward an Edmunds Optics plano-convex lens with 50 mm diameter and back focal length of 247 mm. Its purpose is to focus photons upon the PMT located at the end of the lens tube. Figure 3 shows a 2-D diagram of the detection cube and chamber.

The mirror and lenses are placed as best as possible to utilize their optical characteristics. The source of fluorescence photons is taken to be where the TaO molecule beam and excitation laser intersect within the detection cube. Therefore, the reflector mirror is placed 50 mm away from the intersection to make it two times its focal length from the fluorescence source. Incident photons then reflect back at the same direction toward the condenser lens, minimizing the number of photons lost. Similarly, the condenser lens is placed such that its back focal length of 24.7 mm ends at the fluorescence source. Consequently, incident photons are transmitted on a parallel path toward the convex lens. Reflected photons are also collimated, but not as effectively because they often strike at angles normal to the lens surface.

The collimation of photons improves the effectiveness of their focus onto the PMT. Because of length limitations within the vacuum chamber, the PMT is not placed at the end of the convex lens' back focal length. Rather, it is placed approximately 128 mm away. But the PMT window is large enough that focusing from the convex lens is sufficient that all transmitted photons are assumed to strike the PMT. Approximate optical component distances are shown in Fig. 3. Figure S1 shows the final SolidWorks design.

These mirrors and lenses increase the solid angle covered by the PMT, meaning more fluorescence photons impinge upon it. The solid angle is estimated by applying Eq. 5 to the reflector mirror and condenser lens, then summing the two results. The reflector mirror solid angle is $\frac{\pi}{4} \pm 0.04$ sr and condenser lens solid angle is 3.22 ± 0.29 sr. The total solid angle is then 4.01 ± 0.29 sr. Experimental solid angle efficiency is then calculated by dividing the experimental solid angle by the maximum solid angle of 4π, yielding 31.87%.

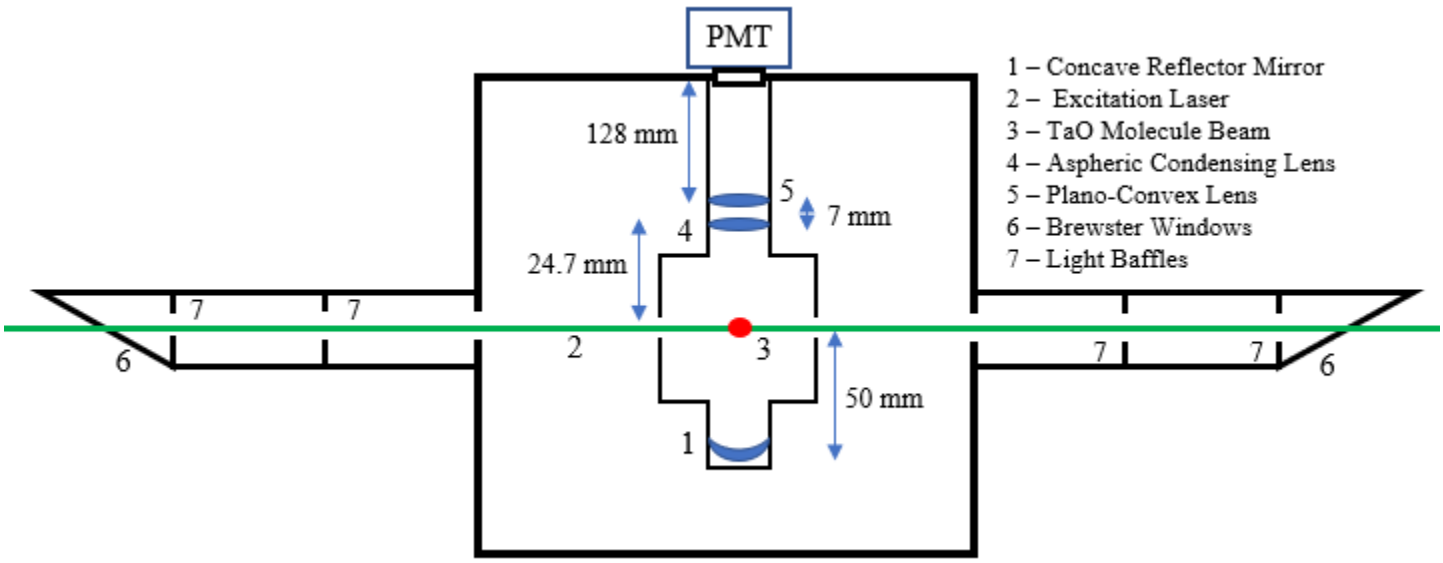

FIG. 3. Diagram of detection chamber and detection cube. Includes relevant distances of optical components.

Experimental detection loss occurs at each interface of the entry Brewster window, reflector mirror, lenses, and PMT window. In total, each of these eight interfaces are assumed to have 5% photon loss, totalling 40%. The reflector mirror has average reflectance of 90%, meaning 10% of photons are lost. Thus, overall detection loss from optical components is 50%.

B. Scattering Reduction

The laser enters and exits the detection chamber via two transparent windows placed at ends of stainless-steel tubes connected to the chamber. Significant scattering of laser photons occurs as the laser enters and exits the two windows. These scattered photons could directly travel or reflect into the detection chamber and possibly be detected by the PMT. As discussed earlier, the expected energy of the excitation laser pulse is approximately 10 μJ, producing 10^{13} photons per shot, but the number of fluorescence photons detected by the PMT is only around 30 per shot. Therefore, even a small fraction of excitation laser photons entering the PMT would completely dominate the fluorescence signal. Normally, a long-pass filter is used to block scattered laser excitation photons, enabling detection of red-shifted fluorescence photons. But a filter cannot be used in the experiment as it blocks fluorescence photons from transitions to lower energy or ground states and must be changed often when conducting a broadband survey spectra of TaO. Thus, various other methods are implemented into the experiment to reduce noise from scattered laser photons.

The first method is painting the inside of the detection chamber with black, graphite aerosol that is vacuum compatible. Secondly, the transparent windows are oriented at the Brewster angle relative to the incident laser. The Brewster angle ensures that all p-polarized light is transmitted without reflection at the surfaces of the window. Third, light baffles are placed between the Brewster windows and detection chamber within the tubes, as shown in Fig. 3. Light baffles are used to block scattered photons produced at the Brewster windows which contain imperfections, such as contamination spots or air bubbles. Baffles are pieces of metal which block all photons except for a small opening which the laser travels through. The size of the opening must not be so small that it diffracts the laser or interferes with its path. Thus, the opening diameter is a balance between preventing interference of the excitation laser and preventing scattered photons from entering the detection chamber.

Lastly, the most important method involves implementing a fast PMT gate switch to block the pulse of scattered photons from each laser pulse. More detail regarding the fast gate switch is described in the following section. In total, these methods are expected to reduce the number of counted scattered photons to below one per laser shot. Confirming this expectation via experiment is currently in progress.

C. PMT Gate Switching and Noise

Initially, a Photek PMT240 was going to be used for photon detection. It has two micro-channel plates with typical gain of $1{\cdot}10^6$, meaning a single photon would produce 34.8 mV signals with typical 230 ps pulse rise time and input impedance of 50 Ω in accordance with Eq. 6. Input impedance is 50 Ω for maximum photon counting resolution. If necessary, signal would be amplified by a Stanford Research Systems SR445 fast preamplifier. Most importantly, the Photek PMT240 possessed a fast gating capability of up to 2 ns. Therefore, the PMT could be gated on and off by inputting TTL signals with the desired pulse time.

However, after conditioning the Photek PMT240 by slowly

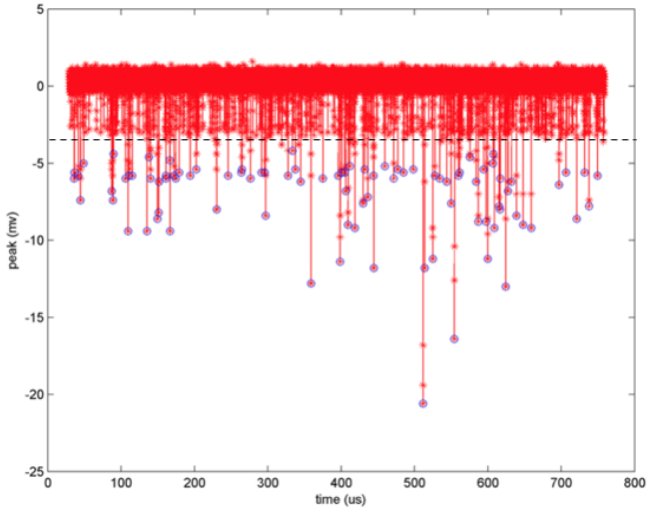

FIG. 4. An example of LIF signal that photon counting would be applied to. Dotted black line represents threshold signal must be greater than to be counted. This plot is an example only and is not from this lab or a simulation.

applying negative voltage via the EMCO C50N power supply, it was found to be completely unresponsive. It failed to report any signal, even when exposed to ambient light of the room. And because the system is highly sensitive and vacuum sealed, it could not be inspected to possibly resolve the issue. Thus, a dynode Hamamatsu R3896 PMT, with typical gain of $9.5{\cdot}10^6$ and 2.2 ns pulse rise time, was chosen for photon detection. Its typical photocathode efficiency is between 14% and 30%. However, the R3896 PMT lacks built-in gating abilities, necessitating the construction of a fast-gating circuit.

The first thought is to design a gating circuit that turns power of all nine PMT dynodes on and off. However, this was impractical as the time it takes for all dynodes to discharge and stop reporting signal is slow, about 100 ns. For example, the RC time constant of a single dynode, $\tau = R \cdot C$, determines the time it takes for the dynode's capacitor to discharge through a resistor. Because the R3896 PMT utilizes high voltage, up to -1 kV, large voltage divider resistors (>10 kΩ) are used. Additionally, total capacitance of the dynodes is greater than 10 pF. Thus, the time constant of the RC circuit is in excess of 100 ns, meaning it takes at least 100 ns seconds for a PMT to discharge enough that it blocks signal. But the excitation laser will pulse at several ns, so the PMT would detect considerable noise from excitation laser photons. Thus, the time it takes for all dynodes to discharge and stop the electron cascading effect is orders of magnitude larger than the time scale needed to switch the gate on and off.

The solution to this discharging issue is to target the first dynode for gating. The fast-gating circuit works by applying a positive electric field to the first dynode which opposes the motion of generated photoelectrons. As a result, no photoelectrons reach the first dynode, the cascading effect cannot begin, and no signal is detected by the anode. All other dynodes retain their potentials, but they receive no photoelectrons to begin the cascading effect due to the first dynode's repulsive field. The total resistance and capacitance is reduced by a factor of ten, and the gate switching time can be reduced to a nano second scale.

The circuit in Fig. 5 gates PMT signal through switches on the first and second dynode to improve total percentage of blocked excitation photons but maintain fast gating. When activated, it works by quickly discharging power from dynode one and dynode two through R7 and R1, respectively. It will be applied to the R3896 PMT and is expected to reach gate switching times of several ns and reduce scattered photons by $1{\cdot}10^8$ per shot, effectively making noise less than one photon per shot, within a 10 μs experimental time frame.

Typical dark current of the Hamamatsu R3896 is 10 nA, and when combined with inherent noise of the oscilloscope noise, total noise is about 1 mV. Intrinsic equipment noise from the PMT and oscilloscope is accounted for by photon counting techniques during data analysis.

D. Photon Counting

Dark current, equipment noise, and fluctuations of detector response are removed when analyzing signal through proper photon counting. A balance between signal height and width must be implemented in input impedance to effectively discern signals. Resulting signal is plotted with peak voltage on the y-axis and time on the x-axis. An arbitrary example of LIF signal is shown in Fig. 4. Electronic noise are the persistent small amplitude fluctuations near zero and the many peaks that only reach approximately -2.5 mV. Therefore, the noise is eliminated by applying a threshold signal peak for counting.

All signal which meets or exceeds the peak threshold is counted as a fluorescence photon. In Fig. 4, this threshold would be set at 3 mV and is indicated by a black line. However, correctly setting the threshold is important, as some jumps in voltage can be noise fluctuations. Improving the signal's peak voltage facilitates photon counting as there is larger separation between signal and noise. Increasing gain is the most direct way to do this but changing input impedance can also affect the signal peak. Inevitably, false signals are recorded over the threshold and are subsequently counted as photons. Photon counting is also unable to discern when two photons are detected by the PMT simultaneously, and they will be counted as one photon.

V. INTERPRETATION AND CONCLUSIONS

The final estimation that the number of counted photons per shot is 30 compared to the $1{\cdot}10^4$ number of atoms which populate the targeted energy state indicates overall efficiency of fluorescence detection is strikingly low. Inherent inefficiencies in optical components, excitation, and PMT detection reduce final signal by several orders of magnitude. Even creating a detection cube system to optimize solid angle coverage is unable to appreciably increase the number of photons detected. The photon counting rate would increase as the exper-

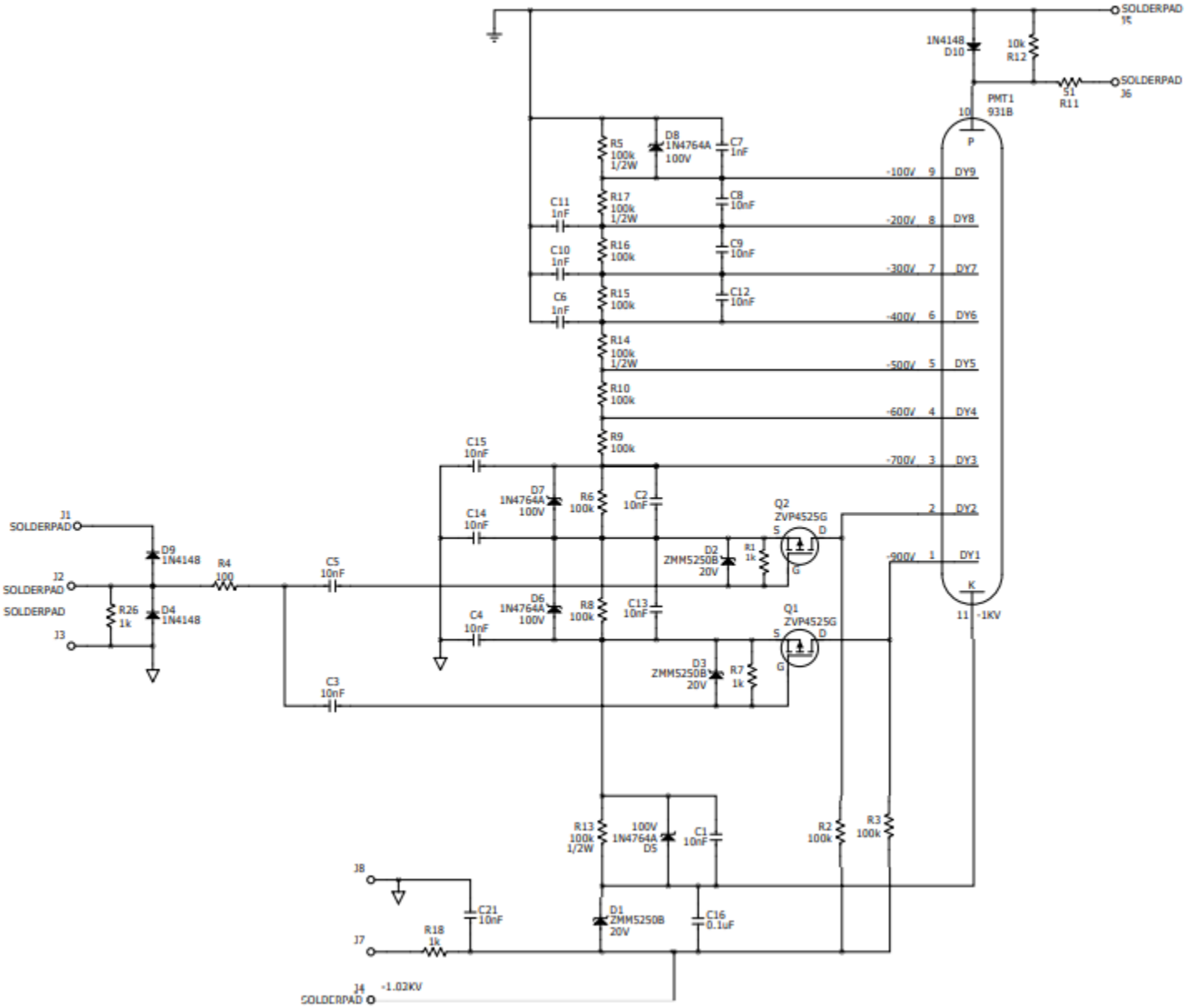

FIG. 5. Fast gating circuit. Dynode 1 (DY1) and dynode 2 (DY2) are gated. Switches Q1 and Q2 control gating. Dynode power drains quickly through R7 and R1. Circuit credit of T. Brown from JILA electronics lab.

iment is conducted, where the molecular number and excitation efficiency are optimized. It is believed that typical molecular number could be increased to at least $1{\cdot}10^5$, increasing detected fluorescence photons by an order of magnitude.

The number of scattered photons which introduce noise is orders of magnitude larger than fluorescence signal detected, posing an enormous obstacle in acquiring useful data. Gating the PMT detector is the most effective way to reduce the noise produced from scattered excitation laser photons, as it reduces the number of scattered photons by several orders of magnitude. Ultimately, the expected noise from background scattering is less than one photon per shot, within a 10 μs detection frame, resulting in a signal-to-background ratio of 30 to one.

[1] W. Demtröder, *Laser Spectroscopy 1: Basic Principles*, 5th ed. (Springer, 2014).
[2] R. C. Hillborn, "Einstein coefficients, cross sections, f values, dipole moments, and all that," American Journal of Physics **50**, 982 (1982).
[3] W. Demtröder, *Laser Spectroscopy 2: Experimental Techniques*, 5th ed. (Springer, 2015).
[4] J. R. Taylor, *Classical Mechanics* (University Science Books, 2005).
[5] J. R. Lakowicz, *Principles of Fluorescence Spectroscopy*, 3rd ed. (Springer, 2006).
[6] Hamamatsu, *Photomultiplier Tubes: Basics and Applications*, 3rd ed. (Hamamatsu Photonics, 2007).
[7] K. Bergmann *et al.*, "Power broadening revisted: theory and experiment," Optics Communications **199**, 117 (2001).

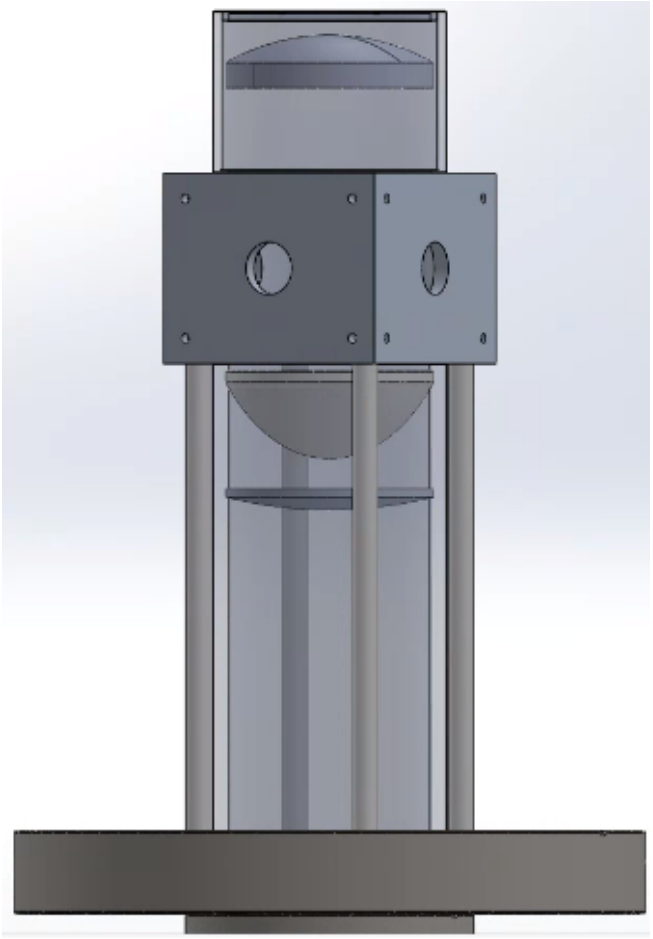

FIG. S1. SolidWorks design of detection cube.

Appendix A: Supplemental Figures